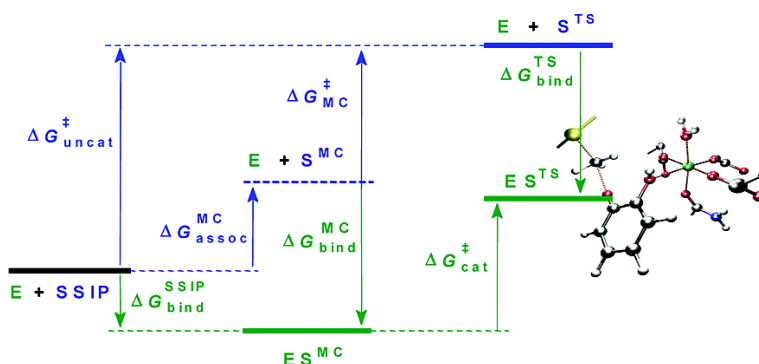


## Theoretical Modeling of Enzyme Catalytic Power: Analysis of “Cratic” and Electrostatic Factors in Catechol O-Methyltransferase

Maita Roca, Sergio Mart, Juan Andrs, Vicent Moliner, Iaki Tun, Juan Bertrn, and Ian H. Williams

*J. Am. Chem. Soc.*, **2003**, 125 (25), 7726-7737 • DOI: 10.1021/ja0299497 • Publication Date (Web): 29 May 2003

Downloaded from <http://pubs.acs.org> on March 29, 2009



### More About This Article

Additional resources and features associated with this article are available within the HTML version:

- Supporting Information
- Links to the 12 articles that cite this article, as of the time of this article download
- Access to high resolution figures
- Links to articles and content related to this article
- Copyright permission to reproduce figures and/or text from this article

[View the Full Text HTML](#)

## Theoretical Modeling of Enzyme Catalytic Power: Analysis of “Cratic” and Electrostatic Factors in Catechol O-Methyltransferase

Maite Roca,<sup>†</sup> Sergio Martí,<sup>†</sup> Juan Andrés,<sup>†</sup> Vicent Moliner,<sup>\*,†</sup> Iñaki Tuñón,<sup>\*,‡</sup>  
Juan Bertrán,<sup>§</sup> and Ian H. Williams<sup>||</sup>

Contribution from the Departament de Ciències Experimentals, Universitat Jaume I, Box 224, 12080 Castellón, Spain, Departament de Química Física, Universidad de Valencia, 46100 Burjasot, Valencia, Spain, Departament de Química, Universitat Autònoma de Barcelona, 08193 Bellaterra, Barcelona, Spain, and Department of Chemistry, University of Bath, BA2 7AY Bath, United Kingdom

Received December 28, 2002; E-mail: moliner@exp.uji.es; Ignacio.Tunon@uv.es

**Abstract:** A comparative theoretical study of a bimolecular reaction in aqueous solution and catalyzed by the enzyme catechol O-methyltransferase (COMT) has been carried out by a combination of two hybrid QM/MM techniques: statistical simulation methods and internal energy minimizations. In contrast to previous studies by other workers, we have located and characterized transition structures for the reaction in the enzyme active site, in water and in a vacuum, and our potential of mean force calculations are based upon reaction coordinates obtained from features of the potential energy surfaces in the condensed media, not from the gas phase. The AM1/CHARMM calculated free energy of activation for the reaction of S-adenosyl methionine (SAM) with catecholate catalyzed by COMT is 15 kcal mol<sup>-1</sup> lower than the AM1/TIP3P free-energy barrier for the reaction of the trimethylsulfonium cation with the catecholate anion in water at 300 K, in agreement with previous estimates. The thermodynamically preferred form of the reactants in the uncatalyzed model reaction in water is a solvent-separated ion pair (SSIP). Conversion of the SSIP into a contact ion pair, with a structure resembling that of the Michaelis complex (MC) for the reaction in the COMT active site, is unfavorable by 7 kcal mol<sup>-1</sup>, largely due to reorganization of the solvent. We have considered alternative ways to estimate the so-called “cratic” free energy for bringing the reactant species together in the correct orientation for reaction but conclude that direct evaluation of the free energy of association by means of molecular dynamics simulation with a simple standard-state correction is probably the best approach. The latter correction allows for the fact that the size of the unit cell employed with the periodic boundary simulations does not correspond to the standard state concentration of 1 M. Consideration of MC-like species allows a helpful decomposition of the catalytic effect into preorganization and reorganization phases. In the preorganization phase, the substrates are brought together into the MC-like species, either in water or in the enzyme active site. In the reorganization phase, the roles of the enzymic and aqueous environments may be compared directly because reorganization of the substrate is about the same in both cases. Analysis of the electric field along the reaction coordinate demonstrates that in water the TS is destabilized with respect to the MC-like species because the polarity of the solute diminishes and consequently the reaction field is also decreased. In the enzyme, the electric field is mainly a permanent field and consequently there is only a small reorganization of the environment. Therefore, destabilization of the TS is lower than in solution, and the activation barrier is smaller.

### Introduction

Enzymes are biological catalysts that are capable of speeding up chemical processes as compared with the related reactions in solution.<sup>1</sup> While this fact is clear, the way these catalysts work is still under debate. Following the seminal idea of Pauling

related to enzyme catalysis,<sup>2</sup> Warshel proposed that the preferential stabilization of the transition state (TS) is essentially electrostatic in nature, due to the favorable organization of the charge distribution in the enzyme active site.<sup>3</sup> In contrast, electrostatic stabilization of the TS in solution involves energetically costly reorganization of solvent molecules, evaluated as half of the solvent–solute interaction energy when using continuum models of solvated systems.<sup>4</sup> However, in going from

<sup>†</sup> Universitat Jaume I.

<sup>‡</sup> Universidad de Valencia.

<sup>§</sup> Universitat Autònoma de Barcelona.

<sup>||</sup> University of Bath.

(1) (a) Fersht, A. *Enzyme Structure and Mechanism*; W. H. Freeman and Company: New York, 1985. (b) Jencks, W. P. *Adv. Enzymol.* **1975**, *43*, 219–410.

(2) (a) Pauling, L. *Chem. Eng. News* **1946**, *24*, 1375–1377. (b) Pauling, L. *Nature* **1948**, *161*, 707–709.

(3) (a) Warshel, A. *P. Natl. Acad. Sci. U.S.A.* **1978**, *75*, 5250–5254. (b) Warshel, A. *J. Biol. Chem.* **1998**, *273*, 27035–27038.

reactants to TS in an enzyme active site, favorable enzyme–substrate interactions are achieved without significant reorganization of the environment. The enzymic charge distribution preferentially stabilizes the TS of the catalyzed reaction relative to reactants with a much-reduced energetic cost.

However, reorganization of the enzyme is not the only factor contributing to enzyme catalytic power. The ability of an enzyme to bind substrate(s) in the Michaelis complex (MC) with an appropriate conformation capable of progressing to the TS can be an important component of catalysis. Menger,<sup>5</sup> Bruice,<sup>6</sup> and Koshland<sup>7</sup> have explained enzyme catalysis by focusing on a variety of factors contributing to formation of the MC and to its possible destabilization in solution. They consider that bringing the reactant fragments to an adequate distance and orientation is mainly an enthalpic term. Westheimer,<sup>8</sup> and later Page and Jencks,<sup>9</sup> pointed out that an enzyme could catalyze a bimolecular reaction by serving simply as an “entropy trap”: the unfavorable entropy of association of the substrates could be “paid for” by favorable binding interactions within the MC, thereby in effect making the reaction unimolecular. Following this direction, Hermans and Wang<sup>10</sup> presented a complete treatment for calculating free energies of formation of macromolecule–ligand complexes and, more recently, Kollman and co-workers<sup>11</sup> considered the implications of bringing the molecules together and of orienting them properly: in most cases a free-energy price must be paid to form a reactant complex in solution, while in the enzyme the substrate binding energy associated to the formation of the MC (and thus its dissociation constant  $K_m$ ) includes the free-energy price for entropic and desolvation contributions. Finally, Warshel and co-workers<sup>3b,12</sup> have presented an approach to evaluate the entropic contribution to the activation barrier of an enzymatic reaction and of the corresponding reference reaction in solution. In this view of enzyme catalysis, the emphasis is made on the *preorganization* of the substrate in a particular conformation prepared to progress up to the corresponding TS.

As part of a research program to evaluate these possible key factors in enzyme catalysis, we have previously studied<sup>13</sup> a unimolecular reaction, the conversion of (–)-chorismate to

prephenate catalyzed by *Bacillus subtilis* chorismate mutase (BsCM) by means of hybrid quantum-mechanical/molecular-mechanical (QM/MM) and molecular dynamics (MD) methods to compute the potential of mean force (PMF)<sup>14</sup> along a suitable reaction coordinate. Being unimolecular, this reaction avoided the problem of bringing separate reactant fragments together to an appropriate distance and orientation, so simplifying this aspect into a conformational issue. This study concluded that reorganization of the enzyme and preorganization of the substrate were not independent factors but were both consequences of the favorable structure of the enzyme for catalysis.

To check these conclusions derived from a unimolecular reaction, we now present an analogous study of a bimolecular reaction, namely methyl transfer from *S*-adenosylmethionine (SAM) to the hydroxylate oxygen of a substituted catechol catalyzed by catechol *O*-methyltransferase (COMT, EC 2.1.1.6).<sup>15</sup> COMT is important in the central nervous system where it metabolizes dopamine, adrenaline, noradrenaline, and various xenobiotic catechols. One important substrate for COMT is levodopa, presently the most effective drug for Parkinson’s disease.<sup>16</sup> This reaction involves attack on a methyl group, originally bonded to the sulfur atom of the coenzyme SAM, by a catecholate O<sup>–</sup> in a direct bimolecular S<sub>N</sub>2 process that can be formally considered as an inverse Menschutkin reaction where ionic reactants proceed toward neutral products.<sup>17–19</sup> The enzymatic process also requires the presence of a magnesium cation (Mg<sup>2+</sup>) in the active site. We have selected this enzymatic system because it possesses some advantages: (i) the results of the reaction catalyzed by the enzyme COMT can be compared with a similar process in solution, with experimental data available in the literature; (ii) the cofactor and the substrate are the only reactants, while the protein environment does not directly take part into the reaction; (iii) no covalent bonds are formed between the substrate and the protein, and therefore, technical problems of frontier treatments between QM and MM regions are avoided.

Recently, Bruice and co-workers carried out both QM and MD calculations relevant to the reaction catalyzed by COMT.<sup>6a,19</sup> They studied the reaction of (CH<sub>3</sub>)<sub>3</sub>S<sup>+</sup> with catecholate anion (catO<sup>–</sup>) in the gas phase and in water treated with continuum solvent models and pointed out the important role of desolvation for this reaction.<sup>19a</sup> From their MD calculations, they concluded that the methyl of SAM and the O<sup>–</sup> of catechol were in a “near attack configuration” (NAC) for a large fraction of the time; moreover, little structural rearrangement of the enzyme was needed to occur between an NAC and the TS.<sup>19c</sup> On the basis of QM supermolecule calculations, they asserted that catalysis did not arise from preferential interactions of the TS with the enzyme but rather from orienting the reactants into an NAC.<sup>19b</sup> However, they did not directly study the energetics of the

- (4) (a) Cramer, C. J.; Truhlar, D. G. *Chem. Rev.* **1999**, *99*, 2161–2200. (b) Cramer, C. J.; Truhlar, D. G. In *Solvent Effects and Chemical Reactivity*; Tapia, O., Bertrán, J., Eds. Kluwer: Dordrecht, The Netherlands, 1996; pp 1–80.
- (5) (a) Menger, F. M. *Acc. Chem. Res.* **1993**, *26*, 206–212. (b) Khanjin, N. A.; Snyder, J. P.; Menger, F. M. *J. Am. Chem. Soc.* **1999**, *121*, 11831–11846.
- (6) (a) Lau, E. Y.; Bruice, T. C. *J. Am. Chem. Soc.* **1998**, *120*, 12387–12394. (b) Torres R. A.; Schiøt B.; Bruice T. C. *J. Am. Chem. Soc.* **1999**, *121*, 8164–8173. (c) Lightstone, F. C.; Bruice, T. C. *J. Am. Chem. Soc.* **1996**, *118*, 2595–2605. (d) Bruice, T. C.; Lightstone, F. C. *Acc. Chem. Res.* **1999**, *32*, 127–136. (e) Bruice, T. C.; Benkovic, S. J. *Biochemistry* **2000**, *39*, 6267–6274. Bruice, T. C. *Acc. Chem. Res.* **2002**, *35*, 139–148.
- (7) Mesecar, A. T.; Stoddard, B. L.; Koshland, D. E. *Science* **1997**, *227*, 202–206.
- (8) Westheimer, F. H. *Adv. Enzymol.* **1962**, *24*, 441–482.
- (9) Page, M. I.; Jencks, W. P. *Proc. Natl. Acad. Sci. U.S.A.* **1971**, *68*, 1678.
- (10) Hermans, J.; Wang, L. *J. Am. Chem. Soc.* **1997**, *119*, 2707–2714.
- (11) (a) Stanton, R. V.; Peräkylä, M.; Bakowies, D.; Kollman, P. A. *J. Am. Chem. Soc.* **1998**, *120*, 3448–3457. (b) Kollman, P. A.; Kuhn, B.; Donini, O.; Peräkylä, M.; Stanton, R. V.; Bakowies, D. *Acc. Chem. Res.* **2001**, *34*, 72–79.
- (12) Villà, J.; Strajbl, M.; Glennon, T. M.; Sham, Y. Y.; Chu, Z. T.; Warshel, A. P. *Natl. Acad. Sci. U.S.A.* **2000**, *97*, 11899–11904.
- (13) (a) Martí, S.; Andrés, J.; Moliner, V.; Silla, E.; Tuñón, I.; Bertrán, J. *Theor. Chem.* **2001**, *105*, 207–212. (b) Martí, S.; Andrés, J.; Moliner, V.; Silla, E.; Tuñón, I.; Bertrán, J. *J. Phys. Chem. B.* **2000**, *104*, 11308–11315. (c) Martí, S.; Andrés, J.; Moliner, V.; Silla, E.; Tuñón, I.; Bertrán, J.; Field, M. J. *J. Am. Chem. Soc.* **2001**, *123*, 1709–1712. (d) Martí, S.; Andrés, J.; Moliner, V.; Silla, E.; Tuñón, I.; Bertrán, J. P. *Chem.–Eur. J.* **2003**, *9*, 984–991. (e) Martí, S.; Andrés, J.; Moliner, V.; Silla, E.; Tuñón, I.; Bertrán, J. P. *THEOCHEM*, in press.

- (14) Roux, B. *Comput. Phys. Commun.* **1995**, *91*, 275–282.
- (15) Takusagawa, F.; Fujioka, M.; Spies, A.; Schowen, R. L. In *Comprehensive Biological Catalysis*; Sinnott, M., Ed.; Academic Press: San Diego, CA, 1998; Vol. 1, pp 1–30.
- (16) Gulberg, H. C.; Marsden, C. A. *Pharmacol. Rev.* **1975**, *27*, 135–206.
- (17) (a) Hegazi, M. F.; Borchardt, R. T.; Schowen, R. L. *J. Am. Chem. Soc.* **1979**, *101*, 4359–4365. (b) Rodgers, J.; Femece, D. A.; Schowen, R. L. *J. Am. Chem. Soc.* **1982**, *104*, 3263–3268.
- (18) (a) Woodard, R. W.; Tsai, M. D.; Floss, H. G.; Crooks, P. A.; Coward, J. K. *J. Biol. Chem.* **1980**, *255*, 9124–9127. (b) Knipe, J. O.; Vasquez, P. J.; Coward, J. K. *J. Am. Chem. Soc.* **1982**, *104*, 3202–3209.
- (19) (a) Zheng, Y. J.; Bruice, T. C. *J. Am. Chem. Soc.* **1997**, *119*, 8137–8145. (b) Kahn, K.; Bruice, T. C. *J. Am. Chem. Soc.* **2000**, *122*, 46–51. (c) Lau, E. Y.; Bruice, T. C. *J. Am. Chem. Soc.* **2000**, *122*, 7165–7171.

enzyme-catalyzed reaction including the protein environment, nor did they perform comparable studies for the uncatalyzed reaction in water. Kuhn and Kollman (KK)<sup>20</sup> used a combined QM and free-energy approach to calculate an activation free energy of 24.5 kcal mol<sup>-1</sup> for the enzymatic reaction, in reasonable agreement with the experimental value<sup>21</sup> of 18 kcal mol<sup>-1</sup>. KK calculated an activation free energy for the reaction between a complex between (CH<sub>3</sub>)<sub>3</sub>S<sup>+</sup> and catO<sup>-</sup> in water, having a structure resembling the MC, and obtained a value 5 kcal mol<sup>-1</sup> higher than for the enzymatic reaction. Addition of (what they called) a “cratic” free-energy term, estimated at 9–13 kcal mol<sup>-1</sup>, improved the agreement between the calculated and experimental rate enhancements for the enzymatic reaction over the uncatalyzed model reaction in water. However, it is important to point out that their treatment, based on gas-phase entropies and assuming arbitrarily the configurational volume in the enzyme, drastically overestimates the entropy changes in solution, as previously mentioned by Warshel and co-workers.<sup>22</sup> There is also an important difference between these studies concerning the coordination of the magnesium cation: in KK’s model,<sup>20</sup> the Mg<sup>2+</sup> is monocoordinated to the catecholate O<sup>-</sup>, but in Bruice’s model,<sup>19c</sup> it interacts with both oxygen atoms of the catechol.

The main aim of this work is to present an analysis of the reorganization of the enzyme and the preorganization of the substrate for this S<sub>N</sub>2 enzyme catalyzed reaction. For this purpose, we have run hybrid QM/MM energy optimizations in solution and in the enzyme environment as well as statistical MD simulations following the strategy described in the next section. KK suggested that the two main approximations in their work were uncertainties in estimating reaction-path geometries and in determining the cratic free energy in solution.<sup>20</sup> We consider that this study represents an improvement in both respects. Furthermore, in presenting an analysis of the electrostatic potential provided by the environment, we also pick up upon a theme the importance of which was also stressed by Kollman’s work.<sup>20</sup>

## Methods

To gain insight of the key factors in enzyme catalysis, free-energy profiles for reaction in both the protein environment and aqueous solution are required. We start with the location and characterization of the relevant stationary structures on the potential energy surface (PES) not only for these condensed media but also in a vacuum. Once an appropriate reaction coordinate has been selected, the PMF may be computed.

**Location of Energy Minima and Saddle Points.** We use a combination of the GRACE<sup>23</sup> and CHARMM<sup>24</sup> programs that enables the determination of transition structures for molecular systems with a large number of atoms by means of QM/MM methods. GRACE divides the total coordinate space into two subsets of atoms: a control space in which the Hessian matrix is calculated and a complementary space that does not necessarily match with the QM and MM subsystems. At each Newton–Raphson step of a QM/MM search in the control space, guided by the Hessian, all geometrical coordinates belonging to the

complementary space are minimized. Once a saddle point on the PES is located and characterized, GRACE is capable of tracing the intrinsic reaction coordinate (IRC) paths down to the reactant and product valleys, by means of a modified version of the MOPAC routine based on the method of Gordon and co-workers.<sup>25</sup> From this first stage of our strategy, where we locate a transition structure in the presence of the protein environment or an aqueous medium, analysis of the IRC also allows selection of the appropriate reaction coordinate and determination of the “reactive” reactant structure immediately adjacent to the transition structure. It must be mentioned that these structures can be quite different from those obtained in gas phase, from both the geometrical and electronic points of view. Problems associated with the QM/MM boundary are avoided because the QM region includes the entire cofactor, and substrate and does not involve covalent linkages to any MM atoms.

For the QM/MM enzyme calculations, the initial coordinates were taken from the X-ray crystal structure<sup>26</sup> of a COMT–inhibitor complex with 3,5-dinitrocatechol and the cofactor SAM; the nitro groups were removed, and a catechol OH (the one closer to SAM) was ionized by proton transfer to Lys144. The QM subsystem contained SAM and catO<sup>-</sup> anion (63 atoms), while the remainder of the enzyme, the magnesium cation, waters of crystallization, and solvating water molecules formed the MM subsystem (3365 enzyme atoms plus 285 nonrigid CHARMM-modified TIP3P<sup>27</sup> water molecules). During the QM/MM enzyme optimizations, the QM atoms and the MM atoms lying in a sphere of 17 Å of radius centered on the QM system were allowed to move (a total of 2610 atoms). Optimization steps with GRACE were guided using a Hessian of order 189. The IRC reaction paths were traced down to reactant (R) and product (P) valleys from the saddle points (as described previously<sup>21b</sup>) followed by an optimization of the full system.

To validate our theoretical approach by comparison of calculated results with experimental data reported in the literature for an analogous reaction in aqueous solution, and with previous theoretical studies in a vacuum, we have selected a “small” model (Figure 1) comprising of (CH<sub>3</sub>)<sub>3</sub>S<sup>+</sup> and catO<sup>-</sup>. Calculations in a vacuum were carried out with the GAUSSIAN98 package of programs,<sup>28</sup> with the AM1 semiempirical method,<sup>29</sup> and with ab initio methods based on second-order Møller–Plesset (MP2) perturbation theory<sup>30</sup> using the standard 6-31+G\* basis set. The same small model was employed for the QM/MM calculations in solution: the 26 QM atoms were placed in a cavity deleted from a 17 Å radius sphere of water molecules described by the nonrigid CHARMM-modified TIP3P potential. As the full system was allowed to move, a solvent boundary potential<sup>31</sup> was applied to the resulting 683 MM water molecules in order to maintain its structure at the edges

(20) Kuhn, B.; Kollman, P. A. *J. Am. Chem. Soc.* **2000**, *122*, 2586–2596.

(21) Schultz, E.; Nissinen, E. *Biochem. Pharmacol.* **1989**, *38*, 3953–2956.

(22) Strajbl, M.; Florian, J.; Warshel, A. *J. Phys. Chem. B* **2001**, *105*, 4471–4484.

(23) (a) Moliner, V.; Turner, A. J.; Williams, I. H. *J. Chem. Soc., Chem. Commun.* **1997**, 1271. (b) Turner, A. J.; Moliner, V.; Williams, I. H. *J. Phys. Chem. Chem. Phys.* **1999**, *1*, 1323–1331.

(24) Brooks, B. R.; Brucoleri, R. E.; Olafson, B. D.; States, D. J.; Swaminathan, S.; Karplus, M. *J. Comput. Chem.* **1983**, *4*, 187–217.

(25) (a) Schmidt, M. W.; Gordon, M. S.; Dupuis, M. *J. Am. Chem. Soc.* **1985**, *107*, 2585–2589. (b) Stewart, J. J. P. MOPAC 7, (QCPE 457). *Quantum Chem. Program Exch. Bull.* **1993**, *13*, 42.

(26) Vidgren, J.; Svensson, L. A.; Liljas, A. *Nature* **1994**, *368*, 354–358.

(27) Jorgensen, W. L.; Chandrasekhar, J.; Madura, J. D.; Impey, R. W.; Klein, M. L. *J. Chem. Phys.* **1983**, *79*, 926–935. Note that CHARMM contains a modified TIP3P potential that includes intramolecular terms.

(28) Frisch, M. J.; Trucks, G. W.; Schlegel, H. B.; Scuseria, G. E.; Robb, M. A.; Cheeseman, J. R.; Zakrzewski, V. G.; Montgomery, J. A., Jr.; Stratmann, R. E.; Burant, J. C.; Dapprich, S.; Millam, J. M.; Daniels, A. D.; Kudin, K. N.; Strain, M. C.; Farkas, O.; J. Tomasi; Barone, V.; Cossi, M.; Cammi, R.; Mennucci, B.; Pomelli, C.; Adamo, C.; Clifford, S.; Ochterski, J.; Petersson, G. A.; Ayala, P. Y.; Cui, Q.; Morokuma, K.; Malick, D. K.; Rabuck, A. D.; Raghavachari, K.; Foresman, J. B.; Cioslowski, J.; Ortiz, J. V.; Stefanov, B. B.; Liu, G.; Liashenko, A.; Piskorz, P.; Komaromi, I.; Gomperts, R.; Martin, R. L.; Fox, D. J.; Keith, T.; Al-Laham, M. A.; Peng, C. Y.; Nanayakkara, A.; Gonzalez, C.; Challacombe, M.; Gill, P. M. W.; Johnson, B.; Chen, W.; Wong, M. W.; Andres, J. L.; Gonzalez, C.; Head-Gordon, M.; Replogle, E. S.; Pople, J. A. *Gaussian 98*, revision A.6; Gaussian, Inc.; Pittsburgh, PA, 1998.

(29) Dewar, M. J. S.; Zoebisch, E. G.; Healy, E. F.; Stewart, J. J. P. *J. Am. Chem. Soc.* **1985**, *107*, 3902–3909.

(30) (a) Head-Gordon, M.; Pople, J. A.; Frisch, M. J. *J. Chem. Phys. Lett.* **1988**, *153*, 503–506. (b) Frisch, M. J.; Head-Gordon, M.; Pople, J. A. *J. Chem. Phys. Lett.* **1990**, *166*, 275–280. (c) Frisch, M. J.; Head-Gordon, M.; Pople, J. A. *J. Chem. Phys. Lett.* **1990**, *166*, 281–289.

(31) Brooks, C. L.; Karplus, M. *J. Mol. Biol.* **1989**, *208*, 159–181.

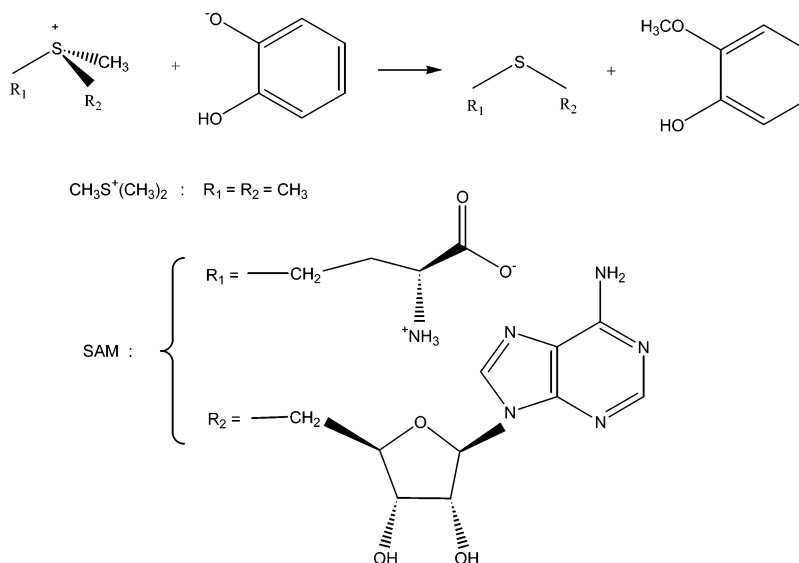


**Figure 1.** Schematic representation of the transmethylation reaction for small and large models.

of the system. Optimization steps for this small model in solution were guided using a Hessian of order 78.

Similar QM/MM calculations were also performed for a "large" model comprising of SAM and  $\text{catO}^-$  (Figure 1). The results obtained with this large model in aqueous medium were compared with the enzymatic data in order to get the necessary information to analyze the factors responsible for enzyme catalysis. The 63 atoms that constituted the large model were treated quantum mechanically and placed in a cavity deleted from a 17 Å radius sphere of nonrigid CHARMM-modified TIP3P water molecules, and a solvent boundary potential was applied to the resulting 659 MM water molecules. Optimization steps for this large model in solution were guided using a Hessian of order 189.

**Potentials of Mean Force.** Study of the PES is complicated because a myriad of minima and saddle point structures are always present when systems with large numbers of degrees of freedom are being considered. Statistical simulations are thus required to obtain averaged properties to be compared with experimental data. The DYNAMO<sup>32</sup> program allows us to obtain the PMF along a single geometrical coordinate or a combination of several. The umbrella-sampling approach is used to constrain the system close to a particular value of the reaction coordinate by means of the addition of a harmonic penalty potential. The probability distributions, obtained from a MD simulation within each individual window, are put together by means of the weighted histogram analysis method (WHAM)<sup>33</sup> to obtain the full probability distribution along the reaction coordinate. It must be pointed out that the simulations are carried out for both the QM and MM regions simultaneously, leading to the change in free energy of the whole system. Selection of a suitable reaction coordinate is essential in order to obtain reliable free-energy differences. In our approach, this choice is made after inspection of the IRCs from the QM/MM PES. It is worth mentioning here the different combined quantum mechanical and free energy QM-FE strategy used by KK<sup>20</sup> to analyze this same reaction: in their study, variations of the MM free energy were calculated by using perturbation theory applied to gas-phase ab initio QM geometrical and charge distributions.

Once the potential energy profiles had been obtained in a vacuum and in the condensed phases (both aqueous and enzymatic), the PMFs were calculated using DYNAMO with periodic boundary conditions. The aqueous-phase system was a cubic box of side 31.4 Å containing

either 1021 water molecules and the small-model solute or 1001 water molecules and the large-model solute. The enzymatic system consisted of a cubic box of side 55.8 Å containing 4614 water molecules and the enzyme (17162 atoms in total). In each case, the QM subsystem comprised  $\text{catO}^-$  and either  $(\text{CH}_3)_3\text{S}^+$  or SAM. Also in each case, the starting geometry was the previously located transition structure, while the reaction coordinate was taken as the antisymmetric combination of the distances describing the breaking and forming bonds, that is,  $D = d_{\text{SC}} - d_{\text{CO}}$  (Figure 1). This variable represented very closely the IRCs that were found in the enzyme, in the gas phase and in solution, and so, it was the natural choice when determining the PMFs. The procedure for the PMF calculation was straightforward and required a series of MD simulations in which the reaction-coordinate variable was constrained about particular values. The different values of the variable sampled during the simulations were then pieced together to construct a distribution function from which the PMF was obtained.

The value of the force constant used for the harmonic umbrella sampling ( $2500 \text{ kJ mol}^{-1} \text{ \AA}^{-2}$  on the reaction coordinate) was determined to allow a full overlapping of the different windows traced in the PMF evaluation, but without losing control over the selected coordinate. Within each window the length of the MD simulation (20 ps) was shown to be long enough to sample a wide range of structures at a reference temperature of 300 K. The canonical thermodynamical ensemble (NVT) was used for all the calculations, thus yielding estimates of the Helmholtz free energy. Changes in the Helmholtz free energy for the condensed-phase reactions considered here are the same as changes in Gibbs free energy, to a good approximation.

Finally, being aware that the AM1 method (used here for the QM region) does not always reproduce reaction barriers very well, we considered the following correction. The in-vacuum energy difference  $\Delta E(\text{MP2}) - \Delta E(\text{AM1})$  was calculated with the MP2/6-31+G\* and AM1 methods for the atoms in the QM region, using averaged structures corresponding to the maximum and minimum of the free-energy profile; this was then added to the AM1/TIP3P computed free-energy barrier for the total system.

**Estimation of Free Energy of Association of Reactants.** Comparison of the calculated free-energy barrier to a bimolecular reaction in water with an experimental free energy of activation requires evaluation of the free-energy change for bringing the reactants together. In the case of a reaction in which charged reactants are transformed into neutral products, this process involves the formation of an ion pair from an isolated, fully solvated cation and anion. This quantity involves a balance of opposing contributions: on one hand, there are

(32) Field, M. J.; Albe, M.; Bret, C.; Proust-de Martin, F.; Thomas, A. *J. Comput. Chem.* **2000**, *21*, 1088–1100.

(33) Torrie, G. M.; Valleau, J. P. *J. Comput. Phys.* **1977**, *23*, 187–199.

**Table 1.** Selected Interatomic Distances and Angles of Transition Structures Optimized in Vacuum, Aqueous, and Enzyme Environments

	trimethylsulfonium + catecholate			SAM + catecholate	
	vacuum		water	water	enzyme
	AM1	MP2	AM1/TIP3P	AM1/TIP3P	AM1/CHARMM
$d_{SC}/\text{\AA}$	1.90	2.13	2.04	1.97	2.01
$d_{CO}/\text{\AA}$	2.22	2.09	2.09	2.17	2.14
SCO/deg	173.4	166.7	173.7	173.7	160.4
$D/\text{\AA}$	-0.32	0.04	-0.05	-0.20	-0.13

unfavorable losses of translational and rotational entropy and of solvation enthalpy, but on the other hand, there are favorable gains in entropy of solvation and cation–anion interaction enthalpy that accompany ion-pair formation. As mentioned above, KK described an approximate procedure for evaluation of the free energy of association for  $(\text{CH}_3)_3\text{S}^+$  and  $\text{catO}^-$  in water to form a species with a MC-like geometry.<sup>20</sup> This energy, which these authors called the “cratic” free-energy contribution, was given as the sum of two terms. The first, which considered changes of solvation energy, solvent entropy, and cavitation energy, was evaluated by means of self-consistent reaction field calculations using Tomasi’s polarized continuum model<sup>34</sup> (PCM) for gas-phase structures of the two separate reactants and of the complex. The second considered the change in solute entropy and was evaluated by means of standard statistical formulas for the partition functions of each species in the ideal gas phase. (Here we may point out that strictly the adjective “cratic” should refer only to the standard-state dependent component involving the change in translational entropy, equivalent to an entropy of mixing;<sup>35</sup> we prefer to consider the overall term simply as a free energy of association.)

A PMF computed for the association of two solute molecules (or in practice the dissociation of their complex) in aqueous solution should provide a correct estimate for the free energy of association, provided that certain conditions are met. The distance between the separated reactant species must be sufficiently large that their motions are independent. However, it must not become so large in relation to the size of the cube of water employed as the unit cell in the periodic-boundary calculations that a species would have unwanted interactions with the image of its partner in a neighboring cell. Furthermore, the simulations must be long enough to allow for adequate sampling of configurations of the complex and of the separated species. Finally, a (genuine) cratic correction to the entropy must be applied to take account of the difference between the concentration of each species in the computer simulations and the standard state concentration of 1 mol  $\text{dm}^{-3}$ . The concentration of a single species in a cubic cell of side 31.4  $\text{\AA}$  (volume  $3.10 \times 10^{-23}$   $\text{dm}^3$ ) is  $5.36 \times 10^{-2}$  mol  $\text{dm}^{-3}$ . Raising the concentration to 1 mol  $\text{dm}^{-3}$  (equivalent to reducing the size of the cell to 11.8  $\text{\AA}$ ) is accompanied by a decrease in entropy of  $R \ln(0.0536)$ ; that is  $\Delta S_{\text{cratic}}(0.0536 \rightarrow 1) = -5.81$  cal  $\text{mol}^{-1}$   $\text{K}^{-1}$ , for each solute species.

## Results and Discussion

Table 1 contains AM1/TIP3P or AM1/CHARMM optimized values for distances  $d_{SC}$ ,  $d_{CO}$ , and  $D = (d_{SC} - d_{CO})$  that defines the reaction coordinate, together with the SCO angle, for transition structures corresponding to first-order saddle points on the PESs for reactions of  $(\text{CH}_3)_3\text{S}^+ + \text{catO}^-$  in a vacuum and in water, and for SAM +  $\text{catO}^-$  in water and in the active site of COMT, Table 2 contains averaged values for the same geometrical parameters for transition states and reactant com-

plexes in water and in the enzyme from QM/MM MD trajectories in the windows corresponding to the minimum and maximum in the PMF. Table 3 contains QM/MM free energies of activation from calculated PMFs.

**Enzyme Environment.** Figure 2 shows the AM1/CHARMM optimized enzymatic transition structure. It is important to note a significant difference in the coordination of the  $\text{Mg}^{2+}$  cation as between the initial geometry and the optimized TS and reactant structures. The former shows coordination of the cation with both O atoms of the  $\text{catO}^-$ , whereas the QM/MM optimized TS shows only one such interaction, between  $\text{Mg}^{2+}$  and the hydroxyl O. Tracing the IRC path down towards the reactant from this saddle point, followed by optimizing the full system, leads to a reactant-like structure that maintains this single  $\text{Mg} \cdots \text{O}$  interaction. This result is not coincident with the one obtained by Kollman et al.<sup>11b,20</sup> starting from the same X-ray structure, followed by MM-MD equilibration and minimization, which showed  $\text{Mg}^{2+}$  coordinated to Asn170, Asp169, a water molecule, the  $\text{O}^-$  of catecholate, and doubly coordinated to Asp141. In their optimized structure, the hydroxyl H atom of catecholate is interacting with Glu199. In contrast, in our optimized structure,  $\text{Mg}^{2+}$  is coordinated to the hydroxyl O atom of the catecholate but not to the  $\text{O}^-$  and to Glu199 (Figure 2). Considering that KK<sup>20</sup> demonstrated that their structure remained stable at 300 K for at least 500 ps, we have also run a QM/MM-MD simulation in order to check the stability of ours. The results confirm that both structures can be considered as different conformers of the reactant state, so in order to change the  $\text{Mg}^{2+}$  coordination much longer MD simulations must be required. Nevertheless, our  $\text{Mg}^{2+}$  coordination pattern offers a catecholate group that is more nucleophilic toward an electrophilic methyl group, whereas the  $\text{Mg}^{2+} \cdots \text{O}^-$  interaction would disfavor this reaction. This result shows the advantage of our strategy of obtaining a “reactive reactant” structure by following the IRC from the transition structure directly to the adjacent energy minimum.

Starting from the saddle points located on the PESs obtained in the enzyme and using  $D$  as the reaction coordinate defined in the previous section led to the PMF shown as the solid line in Figure 3a. This AM1/MM free-energy profile for the enzyme-catalyzed methyl transfer describes a reaction exoergonic by  $\sim 30$  kcal  $\text{mol}^{-1}$  and involving a barrier of 10.4 kcal  $\text{mol}^{-1}$ . The TS from the PMF occurs at  $D = 0.07$   $\text{\AA}$  (Table 2), corresponding to a location slightly later along the reaction coordinate than the transition structure on the PES. The MC from the PMF occurs at  $D = -1.09$   $\text{\AA}$ . Although not presented in the paper, all distances defining magnesium ion coordination are almost equal to the values in Figure 2, except the  $\text{Mg} \cdots \text{OH}$  of catecholate, for which the averaged value is 2.61  $\text{\AA}$ , compared with 2.36  $\text{\AA}$   $D$  for the transition structure on the PES. Application of the MP2 correction to the AM1/CHARMM reaction barrier, using the averaged geometries for MC and TS as described in the previous section, leads to a corrected free-energy barrier  $\Delta G_{\text{corr}}^\ddagger = 20.7$  kcal  $\text{mol}^{-1}$  (Table 3). There is good agreement between this corrected barrier and the experimental<sup>21</sup> free energy of activation (18 kcal  $\text{mol}^{-1}$ ).

**Aqueous and Gaseous Environments.** The distances predicted by AM1 and MP2 for the small model in a vacuum are slightly different (Table 1). The MP2 values are quite close to those obtained by Bruice et al.<sup>19c</sup> at the HF/6-31+G(d,p) level

(34) Miertu, S.; Scrocco, E.; Tomasi, J. *Chem. Phys.* **1981**, *55*, 117–129. (b) Cammi, R.; Tomasi, J. *J. Chem. Phys.* **1994**, *100*, 7495–7502.

(35) (a) Gurney, R. W. *Ionic Processes in Solution*; McGraw-Hill: New York, 1953; pp 88–91. (b) Yu, Y. B.; Privalov, P. L.; Hodges, R. S. *Biophys. J.* **2001**, *81*, 1632–1642.

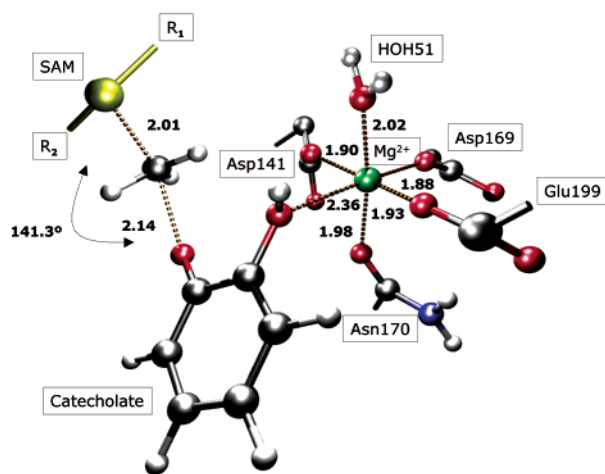
**Table 2.** Averaged Values of Selected Interatomic Distances and Angles of Separated Reactants (R), Reactant Complex (RC), and TS Structures from AM1/MM–MD Simulations in Aqueous and Enzyme Environments

	(CH <sub>3</sub> ) <sub>3</sub> S <sup>+</sup> + catecholate		SAM + catecholate			
	water		water		enzyme	
	R	TS	RC	TS	RC	TS
$d_{SC}/\text{\AA}$	1.82 ± 0.04	2.15 ± 0.05	1.83 ± 0.04	2.12 ± 0.04	1.83 ± 0.04	2.13 ± 0.04
$d_{CO}/\text{\AA}$	6.04 ± 0.69	1.96 ± 0.05	2.94 ± 0.04	2.04 ± 0.04	2.92 ± 0.04	2.06 ± 0.04
SCO/deg	127.4 ± 14.7	169.6 ± 4.9	142.6 ± 9.2	169.6 ± 5.4	138.6 ± 6.5	165.1 ± 5.3
$D/\text{\AA}$	-4.22	0.19	-1.11	0.08	-1.09	0.07

**Table 3.** QM/MM Calculated and Experimental Free-Energy Barriers (kcal/mol)<sup>a</sup>

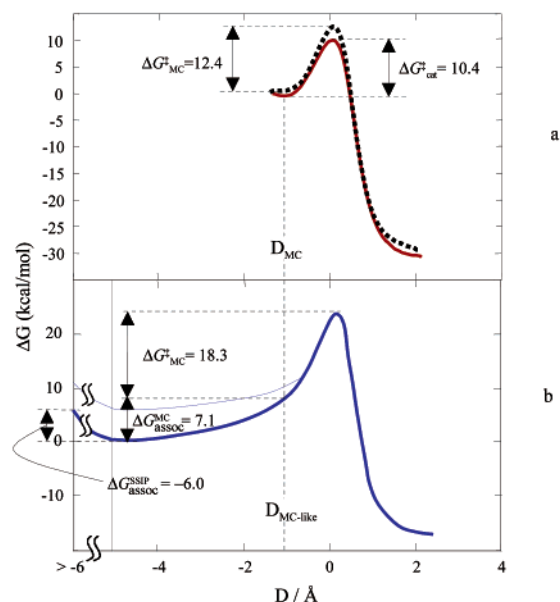
	$\Delta G^\ddagger$	$\Delta G_{\text{corrected}}^\ddagger$	$\Delta G_{\text{exp}}$
enzyme	10.4	20.7	18
water (small model)	25.4	26.9	30.8
water (large model)	12.4	23.5	

<sup>a</sup> The barrier is computed as the free-energy difference between MC and TS, for the enzymatic process, R and TS, for small model in water, and MC-like and TS, for the large model in water.

**Figure 2.** Detail of a transition structure located in the active site of COMT by means of AM1/CHARMM internal energy optimizations.

of theory (2.14 Å for  $d_{SC}$  and 2.16 Å for  $d_{CO}$ ). The aqueous-phase AM1/TIP3P results for this small model indicate a transition structure slightly later along the reaction coordinate (less negative value of  $D$ ) as compared with the gas-phase AM1 method, but the SCO angle is essentially the same (Table 1). Comparison of the small and large models in water shows the transition structure to be slightly earlier for the latter but with the same near-linear SCO angle. The  $d_{SC}$  and  $d_{CO}$  distances for the enzymatic transition structure are similar to those for the aqueous-phase SAM + catO<sup>-</sup> transition structure, but the predicted SCO angle is slightly smaller.

Swain and Taylor<sup>36</sup> reported experimental values of 28.5 kcal mol<sup>-1</sup> and -4.6 cal mol<sup>-1</sup> K<sup>-1</sup>, respectively, for the enthalpy and entropy of activation for (CH<sub>3</sub>)<sub>3</sub>S<sup>+</sup> reacting with the phenolate anion in aqueous solution at 80 °C. If these values are assumed to be not greatly temperature dependent, the free energy of activation at 300 K may be estimated as  $\Delta G^\ddagger = 28.5 - 300 \times (-4.6/1000) = 29.9$  kcal mol<sup>-1</sup>. The difference in nucleophilicity between phenolate and catecholate may be estimated by means of the Brønsted coefficient ( $\beta_{\text{nuc}} \approx 0.3$ ) for nucleophilic attack<sup>37a</sup> and the pK<sub>a</sub> values for phenol (10.0) and

**Figure 3.** QM/MM potentials of mean force computed for (a) the large model in the COMT enzyme (solid line) and in solution (dotted line) and for (b) the small model in aqueous solution. Thinner line corresponds to PMF obtained with constrains (see the text for details).

catechol (9.5);<sup>37b</sup> thus  $\Delta\Delta G^\ddagger = -2.303RT(\beta_{\text{nuc}} \times \Delta\text{p}K_a) = 1.37 \times 0.3 \times (10.0 - 9.5) = 0.2$  kcal mol<sup>-1</sup>. This yields a best estimate of 30.1 kcal mol<sup>-1</sup> for the free energy of activation for (CH<sub>3</sub>)<sub>3</sub>S<sup>+</sup> reacting with catO<sup>-</sup> in aqueous solution at 300 K. For comparison with the results of our PMF calculations, it is necessary to take account of the statistical factor of 3, since our simulations consider reaction at only one of the methyl groups of (CH<sub>3</sub>)<sub>3</sub>S<sup>+</sup>. The barrier to reaction should therefore be raised by  $RT \ln 3$  to give a final value effective experimental free energy of activation for reaction at a single methyl group of 30.8 kcal mol<sup>-1</sup>.

The free-energy profile for (CH<sub>3</sub>)<sub>3</sub>S<sup>+</sup> with catO<sup>-</sup> in water (Figure 3b) shows a reaction exoergonic by ~14 kcal mol<sup>-1</sup> and with a barrier of 25.4 kcal mol<sup>-1</sup> with respect to a solvent-separated ion pair (SSIP) with  $D = -4.22$  Å. The maximum in the PMF corresponds to the TS and occurs at  $D = 0.19$  Å, a position later along the reaction coordinate than the transition structure on the PES with  $D = -0.05$  Å. As  $D$  was decreased from this initial value, so the average value of the SCO angle changed smoothly from 169.6° to ~155° at  $D = -0.7$  Å, after which it was chaotic. To avoid unhelpful sampling of structures with  $D < -0.7$  Å but unrepresentative of the desired reaction path, a constraint was placed upon this angle, and the distance

(37) (a) Coward, J. K.; Sweet, W. D. *J. Org. Chem.* **1971**, *36*, 2337–2346. (b) Paetzel, M.; Dalbey, R. E. *Trends Biochem. Sci.* **1997**, *22*, 28–31. (c) Kenyon, G. L.; Gerlt, J. A.; Petsko, G. A.; Kozarich, J. W. *Acc. Chem. Res.* **1995**, *28*, 178–186.

(36) Swain, C. G.; Taylor L. J. *J. Am. Chem. Soc.* **1962**, *84*, 2456–2457.

$d_{\text{CO}}$  alone was used as the reaction coordinate, leading to the thin line in Figure 3b. However, once a free-energy minimum was reached, corresponding to the SSIP, the constraint was removed, and the full profile (thick line) shown in Figure 3b was obtained by combining the two sections of the PMF. The average value of  $d_{\text{CO}}$  at the free-energy minimum was  $\sim 6 \text{ \AA}$ , and typically there were about three water molecules in the region between the cation and anion. At  $d_{\text{CO}}$  distances longer than  $6 \text{ \AA}$ , the PMF rises toward a value of  $\Delta G \approx 4.3 \text{ kcal mol}^{-1}$  for relative to the SSIP. After correction for the cratic entropy in changing from a concentration of  $5.36 \times 10^{-2} \text{ mol dm}^{-3}$  to  $1 \text{ mol dm}^{-3}$ , the free energy of association of the ions was estimated as  $\Delta G_{\text{assoc}} \approx -6 \text{ kcal mol}^{-1}$ . This value corresponds to an equilibrium constant of  $2.5 \times 10^4$  for formation of the SSIP at 300 K, indicating that this is the thermodynamically favored reactant state in aqueous solution.

Application of the MP2 correction ( $+1.5 \text{ kcal mol}^{-1}$ ) to the AM1/TIP3P small-model reaction barrier, using the averaged geometries for the SSIP and the TS, leads to a corrected free-energy barrier  $\Delta G_{\text{corr}}^{\ddagger} = 26.9 \text{ kcal mol}^{-1}$  (Table 3). This value compares reasonably well with the experimental estimate of  $30.8 \text{ kcal mol}^{-1}$  for the reaction of  $(\text{CH}_3)_3\text{S}^+$  with  $\text{catO}^-$  in water at  $25 \text{ }^\circ\text{C}$  and suggests that the AM1/TIP3P large-model value computed for the free-energy barrier of the corresponding reaction of SAM should also be reasonable.

The TS for the reaction of SAM with  $\text{catO}^-$  corresponds to the maximum in the PMF for the large model in water (Figure 3a, dashed line) which occurs at  $D = 0.08 \text{ \AA}$  (Table 2), a position later along the reaction coordinate than the transition structure on the PES with  $D = -0.20 \text{ \AA}$  (Table 1), the same trend as found for the aqueous small-model reaction. This is a Hammond-effect resulting from stabilization of the ionic reactants, relative to the charge-neutralized products, as a consequence of better solvation on average in the MD simulation than the single reactants structure optimized on the PES. However, the large-model TS has a smaller value of  $D$  than the small-model TS, just as those found for the underlying transition structures on the PES. The average values of the SCO angle (Table 2) for both small- and large-model TSs in aqueous solution are close to optimized values for the transition structures on the PESs (Table 1), just as that found for the enzymatic reaction.

Finally, it may be noted that the change in  $D$  from the SSIP to the TS for the small-model reaction in solution is much larger than the change in  $D$  from the MC to the TS for the enzymatic reaction, consistent with a much larger free-energy barrier. It is important to note that, due to the limitations of size of the cubic box of water molecules, no SSIP was obtained for the large model in water as the two species could not be separated enough. The PMF for the large model in going from TS to reactants was stopped when the solute presented a structure that resembled the MC for the reaction in the COMT active site (no local free-energy minimum was obtained at this point).

**Analysis of ‘‘Cratic’’ Factors.** It has been noted above that several authors have considered the free-energy change for bringing together two reactant molecules in the correct orientation for reaction to occur. In particular, KK<sup>20</sup> estimated this quantity at  $9\text{--}13 \text{ kcal mol}^{-1}$  for the reaction of  $(\text{CH}_3)_3\text{S}^+$  and  $\text{catO}^-$  in water at 300 K, to improve the agreement between calculated and experimental rate enhancements for the enzymatic

reaction over the uncatalyzed model reaction in water. Their estimate was the sum of two components. The first, a free energy of formation for an ion-pair complex in water, was evaluated by means of PCM calculations with the HF/6-31+G method for the ion pair and for the individual cation and anion. Since the coordinates  $d_{\text{SC}}$  and  $d_{\text{CO}}$  in their enzymic MC had values of  $1.82$  and  $2.97 \text{ \AA}$ , respectively, presumably the same values were used to construct the MC-like geometry of the ion pair for the model reaction in water, which they did not explicitly describe. These interatomic distances are very close to the average values (Table 3) obtained from our QM/MM MD simulations for the MC between SAM and  $\text{catO}^-$  in the COMT active site. KK's PCM calculations gave a free-energy change  $\Delta G_{\text{complex}}^*$  (their notation) of  $+3.9 \text{ kcal mol}^{-1}$ ,<sup>20</sup> our own PCM( $\epsilon = 78.4$ )/HF/6-31+G\* evaluation of this component of the free energy of association of  $(\text{CH}_3)_3\text{S}^+$  and  $\text{catO}^-$  in water to form an ion pair with the same geometry as the MC was  $+11.0 \text{ kcal mol}^{-1}$ . In passing, we note that our PCM estimate of  $\Delta G_{\text{complex}}^*$  for the SSIP in water ( $d_{\text{CO}} \approx 6 \text{ \AA}$ ) is only  $+2 \text{ kcal mol}^{-1}$  but also that it is not appropriate to use continuum solvation models in general to treat solvent-separated ion pairs and, in particular, those methods that use a cavity-based approach to the solution of the Poisson equation;<sup>38</sup> we therefore consider these PCM estimates to be of dubious reliability.

The second component, termed  $-T\Delta S_{\text{solute}}$ , was the sum of ideal-gas, rigid-rotor, harmonic-oscillator entropy changes for formation of the same MC-like ion pair; KK reported  $-T\Delta S_{\text{translational}} = +11.1 \text{ kcal mol}^{-1}$ ,  $-T\Delta S_{\text{rotational}} = +6.3 \text{ kcal mol}^{-1}$ , and  $-T\Delta S_{\text{vibrational}} = -8.0 \text{ kcal mol}^{-1}$ . Leaving aside momentarily the issue of whether ideal-gas-phase expressions are appropriate for processes in solution, we obtained (trivially) the same value for the ideal-gas translational entropy change (which depends only on the masses) and essentially the same rotational entropy change ( $-T\Delta S_{\text{rotational}} = +6.4 \text{ kcal mol}^{-1}$ ). It is unclear how KK calculated their vibrational entropy change, since the MC-like ion pair does not correspond to a stationary point on the PES for the model reaction in the gas phase. We have estimated this component in the following way. The vibrational entropy of activation for reaction of  $(\text{CH}_3)_3\text{S}^+$  and  $\text{catO}^-$  in the gas phase, calculated from the AM1 frequencies for the isolated reactant species and the transition structure, is  $-2.1 \text{ cal K}^{-1} \text{ mol}^{-1}$  at 300 K. The vibrational activation entropy accompanying progress from the MC to the transition structure for the COMT-catalyzed reaction was calculated at the AM1/CHARMM level from subset Hessians evaluated for the QM atoms only for these stationary structures. A Hessian for the  $3N - 6$  internal degrees of freedom of each species was obtained by a projection as previously described.<sup>39</sup> This procedure yielded a value for the vibrational entropy of activation of  $-0.4 \text{ cal K}^{-1} \text{ mol}^{-1}$  at 300 K; evidently the MC is a very tight structure that loses very little entropy upon going to the transition state within the COMT active site. Assuming that the small-model reaction would have a similarly small vibrational entropy change as between the MC-like geometry and the transition structure, we obtain our estimate for the vibrational entropy of association of  $(\text{CH}_3)_3\text{S}^+$  with  $\text{catO}^-$  in the gas phase as the difference  $(-2.1) - (-0.4) = -1.7 \text{ cal K}^{-1} \text{ mol}^{-1}$ , from whence  $-T\Delta S_{\text{vibrational}}$

(38) Cramer, C. J. *Essentials of Computational Chemistry: Theories and Models*; Wiley: Chichester, U.K., 2002; p 378.

(39) (a) Williams, I. H. *Chem. Phys. Lett.* **1982**, *88*, 462–466. (b) Williams, I. H. *J. Mol. Struct. THEOCHEM* **1983**, *11*, 275–284.



= +0.5 kcal mol<sup>-1</sup> at 300 K. This value is in marked contrast to KK's estimate of -8.0 kcal mol<sup>-1</sup>;<sup>20</sup> it seems that these authors assumed the ion pair with the MC-like geometry would be a much looser species than our calculations suggest it to be.

At this point, it is worth remarking that, whereas some discussions of entropic contributions to enzyme catalysis<sup>9</sup> have considered vibrational entropy changes to be of negligible importance, KK rightly recognized that six degrees of translational and rotational motion are converted into vibrations in an associative process. According to our estimate, the entropy of these six vibrations in the MC is almost the same as it is in the transition state within the COMT active site.

KK called their sum of  $\Delta G^*_{\text{complex}}$  (3.9 kcal mol<sup>-1</sup>) and  $-T\Delta S_{\text{solute}}$  (9.4 kcal mol<sup>-1</sup>) the "cratic" free energy,  $\Delta G_{\text{cratic}} = +13.3$  kcal mol<sup>-1</sup>. As mentioned above, we consider this term to be a misnomer for the free energy of association, which, according to our estimate, would be about 29 kcal mol<sup>-1</sup> (= 11.0 + 11.1 + 6.4 + 0.5), based upon the ideal-gas approximation. However, in our view, it is unreasonable to consider ions in aqueous solution as if they were noninteracting ideal-gas particles; although each individual solute molecule at a given volume of a solution may (in time) sample exactly the same range of positions and orientations as it could in the same volume of ideal gas, the statistics of the configurations accessible to an ensemble of particles are likely to be quite different, as the result of restrictions upon translational and rotational motion due to intermolecular interactions.

A very simple method<sup>40</sup> to scale a gas-phase entropy in order to estimate approximately the entropy of a solute in water was proposed by Wertz,<sup>41</sup> based upon the observations that the entropy of liquid water at 298 K is 46% less than that of gaseous water at a concentration of 55.5 M and that the entropies of solvation of ammonia, methane, and water in water are almost identical. With the assumptions (which have been criticized<sup>42</sup>) that (a) changes in the entropy of water do not contribute to the entropy of solvation and (b) all molecules lose the same fraction of their entropy when transferred from the gas phase to water, the entropy of solvation  $\Delta S_s$  of any solute (including water) in water at 25 °C may be calculated from the ideal-gas entropy  $S^\circ_g$  of the solute, at 25 °C and 1 atm, by the expression in eq 1.<sup>41</sup> Application of this expression to each component of an ideal-gas system at equilibrium allows the entropy change for the same equilibrium in aqueous solution to be calculated. Conversions of ideal-gas-phase solute entropies to aqueous-phase entropies  $S^+_{\text{aq}}$  at 25 °C and a standard state of 1 M may thus be effected by means of eq 2, leading to eq 3 for the entropy change in a bimolecular association in water.

$$\Delta S_s = -0.46(S^\circ_g - 14.3) \text{ cal K}^{-1} \text{ mol}^{-1} \quad (1)$$

$$S^+_{\text{aq}} = 0.54S^\circ_g + 0.24 \text{ cal K}^{-1} \text{ mol}^{-1} \quad (2)$$

$$\Delta S^+_{\text{aq}} = 0.54\Delta S^\circ_g - 0.24 \text{ cal K}^{-1} \text{ mol}^{-1} \quad (3)$$

Application of eq 2, using  $\Delta S^\circ_g = \Delta S_{\text{translational}} + \Delta S_{\text{rotational}} + \Delta S_{\text{vibrational}} = -60 \text{ cal K}^{-1} \text{ mol}^{-1}$ , provides an (admittedly crude) estimate for  $-T\Delta S_{\text{solute}}$ , corresponding to the loss of the motions

of the cation and anion in forming the ion pair, equal to +9.8 kcal mol<sup>-1</sup> at 300 K. By coincidence, this value is similar to the estimate of KK based upon the unreasonable assumptions of ideal-gas behavior in aqueous solution and of very loose binding in the MC-like ion pair. The entropy of solvation corresponds to transfer of motionless solute molecules from the gas phase to solution;<sup>42b</sup> these changes are implicitly contained in the PCM estimate for  $\Delta G^*_{\text{complex}}$  ( $\approx 11.0$  kcal mol<sup>-1</sup>). Therefore, the overall free energy of association of (CH<sub>3</sub>)<sub>3</sub>S<sup>+</sup> and catO<sup>-</sup> in water at 300 K to form an ion pair with the same geometry as the MC is given by the sum 11.0 + 9.8 = 20.8 kcal mol<sup>-1</sup>.

The AM1/TIP3P calculated PMF for association of (CH<sub>3</sub>)<sub>3</sub>S<sup>+</sup> and catO<sup>-</sup> in water at 300K (Figure 3b) shows a free-energy change of -4.3 kcal mol<sup>-1</sup> for formation of the SSIP, to which should be added the genuine cratic correction  $-T\Delta\Delta S_{\text{cratic}} - (0.0536 \text{ M} \rightarrow 1 \text{ M}) = -300 \times [(-5.81)_{\text{SSIP}} - (-5.81)_{\text{cation}} - (-5.81)_{\text{anion}}] \text{ cal mol}^{-1} = -1.7 \text{ kcal mol}^{-1}$ , giving  $\Delta G_{\text{assoc}}(\text{SSIP}) = -6 \text{ kcal mol}^{-1}$ . Since the AM1/TIP3P calculated free-energy change between the SSIP and the MC-like contact ion pair is +7.1 kcal mol<sup>-1</sup>, the overall estimate for  $\Delta G_{\text{assoc}}(\text{MC})$  from the MD simulations is only about +1 kcal mol<sup>-1</sup>, a value in stark contrast with the estimate of about +21 kcal mol<sup>-1</sup> obtained above by means of a combination of PCM calculations together with estimates of losses in translational and rotational entropy in aqueous solution, and also quite different from the value obtained by KK.<sup>20</sup> Frankly, it appears strange that ion-pair formation should be accompanied by a such a large rise in free energy. In view of the uncertainties discussed above in regard to both aspects of the latter method (which follows KK), we are inclined to prefer the directness of the MD simulation approach. We have obtained a reasonable result, although it should be borne in mind that a definitive energy value for ion-pair formation would require bigger and better calculations than we have yet performed. To evaluate  $\Delta G_{\text{assoc}}(\text{MC})$  for the large model (SAM with catO<sup>-</sup>) would require MD simulations with a dramatically larger box of water molecules and, correspondingly, greater computational requirements. Furthermore, as no experimental data are available for the large model in water, even if we were to run these calculations, we could not check our theoretical predictions.

**Entropies of Activation.** The focus of the previous section was upon the changes free energy and entropy that accompany formation of the MC-like contact ion pair in solution. Now we briefly consider the entropy change from the MC to the transition structure for the COMT-catalyzed reaction and the corresponding change for the reference reaction in water. Above, we have described the procedure followed to estimate the substrate contribution to the vibrational entropy of activation for the enzymatic reaction, giving a very small value of  $\Delta S^\ddagger_{\text{vibrational}} = -0.4 \text{ cal K}^{-1} \text{ mol}^{-1}$  at 300 K. This term includes the six degrees of freedom corresponding to the translational and rotational motions "lost" upon association of SAM with catO<sup>-</sup>. Its small size is consistent with Warshel's observation<sup>12</sup> that motions that are free in the MC are also free in the TS. Note, however, that our estimate does not include the contribution of the protein to  $\Delta S^\ddagger_{\text{vibrational}}$ .

Warshel and co-workers have recently described a restrain-release approach for evaluation of entropy contributions, employing a free-energy perturbation method to estimate the

(40) Williams, I. H.; Spangler, D.; Femec, D. A.; Maggiora, G. M.; Schowen, R. L. *J. Am. Chem. Soc.* **1983**, *105*, 31–40.

(41) Wertz, D. H. *J. Am. Chem. Soc.* **1980**, *102*, 5316–5322.

(42) (a) Abraham, M. H. *J. Am. Chem. Soc.* **1982**, *104*, 2085–2094. (b) Ben-Naim, A.; Marcus, Y. *J. Chem. Phys.* **1984**, *81*, 2016–2027.

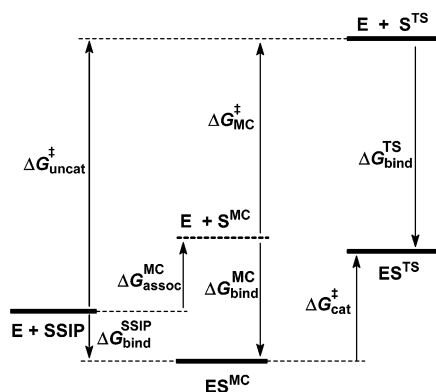


Figure 4. Analysis of contributions to catalysis.

free-energy change resulting from the relaxation of an imposed restraint, such as a restriction upon translational and rotational motion.<sup>43</sup> They have reported very similar values for  $-\Delta\Delta S^\ddagger$  for peptide hydrolysis within an enzyme–substrate complex and within a solvent cage (the equivalent of our MC-like ion pair); these estimates include contributions from both the substrate and its surroundings. This finding provides some support to our assumption (see above) that  $\Delta S^\ddagger_{\text{vibrational}}$  is likely to be similar for both  $\text{MC} \rightarrow \text{TS}$  in COMT and MC-like ion-pair  $\rightarrow \text{TS}$  in water.

**TS Binding and Catalysis.** According to a popular view of enzyme catalytic power, the lower activation energy for a catalyzed reaction, relative to the corresponding uncatalyzed reaction in water, is due to preferential stabilization of the transition state over the substrate;<sup>2</sup> this is equivalent to the difference in binding energies of the species, that is the energy of transfer from water to the enzyme active site. The following relationships are evident from Figure 4.

$$\Delta G_{\text{uncat}}^\ddagger - \Delta G_{\text{bind}}^{\text{SSIP}} = \Delta G_{\text{MC}}^\ddagger + \Delta G_{\text{assoc}}^{\text{MC}} - \Delta G_{\text{bind}}^{\text{SSIP}} = \Delta G_{\text{cat}}^\ddagger - \Delta G_{\text{bind}}^{\text{TS}} \quad (5)$$

$$\Delta G_{\text{uncat}}^\ddagger - \Delta G_{\text{cat}}^\ddagger = \Delta G_{\text{bind}}^{\text{SSIP}} - \Delta G_{\text{bind}}^{\text{TS}} \quad (6)$$

$$\Delta G_{\text{MC}}^\ddagger - \Delta G_{\text{cat}}^\ddagger = \Delta G_{\text{bind}}^{\text{MC}} - \Delta G_{\text{bind}}^{\text{TS}} \quad (7)$$

Equation 6 relates the reduction in free energy of activation for the COMT-catalyzed reaction to the difference in binding energies of the TS and the SSIP. The TS for the reaction of SAM with  $\text{catO}^-$  in water has an average structure very similar to that of the TS for the same reaction in the COMT active site (Table 2), so the binding energy  $\Delta G_{\text{bind}}^{\text{TS}}$  contains very little contribution from substrate reorganization. However, as we have shown above, the SSIP in water is structurally very different from the MC in the enzyme active site, so the term  $\Delta G_{\text{bind}}^{\text{SSIP}}$  contains a significant contribution from substrate reorganization. Both terms involve substantial contributions from solvent reorganization. Equation 7 relates the reduction in free energy of activation to the difference between the binding energies of the TS and the MC, a formulation that invokes the MC-like contact ion pair in water that we have discussed above. Since neither of these are species readily amenable to experimental

characterization, this analysis is purely a formal device to assist our understanding. The advantage of considering the MC-like contact ion pair for the reaction in water is simply that its average structure closely resembles that of the MC for the enzyme catalyzed reaction, so that the term  $\Delta G_{\text{bind}}^{\text{MC}}$  is dominated not by solute deformation but by reorganization of the aqueous and enzymic environments.

In passing, we note that the MC-like species, which corresponds to neither a minimum nor a maximum in the PMF, corresponds broadly to an “NAC” in Bruice’s terminology. In water, this species is unfavorable with respect to the SSIP by  $\Delta G_{\text{assoc}}^{\text{MC}} = 7.1 \text{ kcal mol}^{-1}$  with the consequence that the free-energy barrier  $\Delta G_{\text{MC}}^\ddagger$  is smaller than  $\Delta G_{\text{uncat}}^\ddagger$  by this amount. Conceptually, however, consideration of MC-like species (or NACs) does allow a helpful decomposition of the catalytic effect into preorganization and reorganization phases. In the preorganization phase, the substrates are brought together into the MC-like species, either in water or in the enzyme active site. In the reorganization phase, the roles of the enzyme and aqueous environments may be compared directly because reorganization of the substrate is about the same in both cases. We are in complete agreement with Warshel’s point that the real question concerning enzyme catalysis is how the differential binding is achieved by the enzyme relative to a proper reference state in aqueous solution and to consider this within the context of a proper thermodynamic cycle.<sup>3b</sup>

**Preorganization and Catalysis.** The free energy of association of  $(\text{CH}_3)_3\text{S}^+$  with  $\text{catO}^-$  in water to form a contact ion pair with a structure similar to that of the MC of COMT with SAM and  $\text{catO}^-$  is estimated by means of AM1/TIP3P MD simulations to be  $\sim +1 \text{ kcal mol}^{-1}$ . It seems that formation of the SSIP from the free ions in solution is dominated by the favorable terms previously identified: the enthalpy due to electrostatic attraction between oppositely charged ions and the entropy of desolvation of the individual ions. On the other hand, progress from the loose SSIP to the tight MC-like contact ion pair seems to involve the unfavorable terms noted above, particularly the enthalpy of desolvation. The free energy of association of SAM with  $\text{catO}^-$  to form an MC-like contact ion pair in water is likely to be very similar also. The “price” of the unfavorable free-energy change from the SSIP to this MC-like ion pair in water ( $\Delta G_{\text{assoc}}^{\text{MC}}$  in Figure 4) is “paid for” by the enzyme in the catalyzed process, by virtue of the favorable intrinsic free energy of binding of the latter with COMT.<sup>1b</sup> The preorganized nature of the enzyme allows it to bind SAM and  $\text{catO}^-$  with a resultant free energy ( $\Delta G_{\text{bind}}^{\text{SSIP}}$  in Figure 4) that is smaller than the intrinsic free energy of binding by an amount equal to  $\Delta G_{\text{assoc}}^{\text{MC}}$ .

Figure 5 illustrates the distribution of values for distance  $d_{\text{CO}}$  and angle SCO corresponding to reactant and TS structures in a vacuum, water, and COMT from the dynamical trajectories. These structures were obtained from MD simulation windows corresponding to the maximum and the minimum of the free-energy profile in each medium. It can be readily seen that the distributions for the aqueous and enzymatic TSs are largely overlapping but are distinct from that for the TS distribution in a vacuum. The average value of  $d_{\text{CO}}$  in the condensed-media TSs is (at  $\sim 2.0 \text{ \AA}$ ) shorter than the corresponding value in a vacuum ( $\sim 2.3 \text{ \AA}$ ), thus showing a medium effect as previously

(43) (a) Strajbl, M.; Sham, Y. Y.; Villà, J.; Chu, Z.-T.; Warshel, A. *J. Phys. Chem. B* **2000**, *104*, 4578–4584. (b) Sham, Y. Y.; Chu, Z.-T.; Tao, H.; Warshel, A. *Proteins: Struct., Funct., Genet.* **2000**, *39*, 393–407. (c) Warshel, A.; Parson, W. W. *Q. Rev. Biophys.* **2001**, *34*, 563–679.

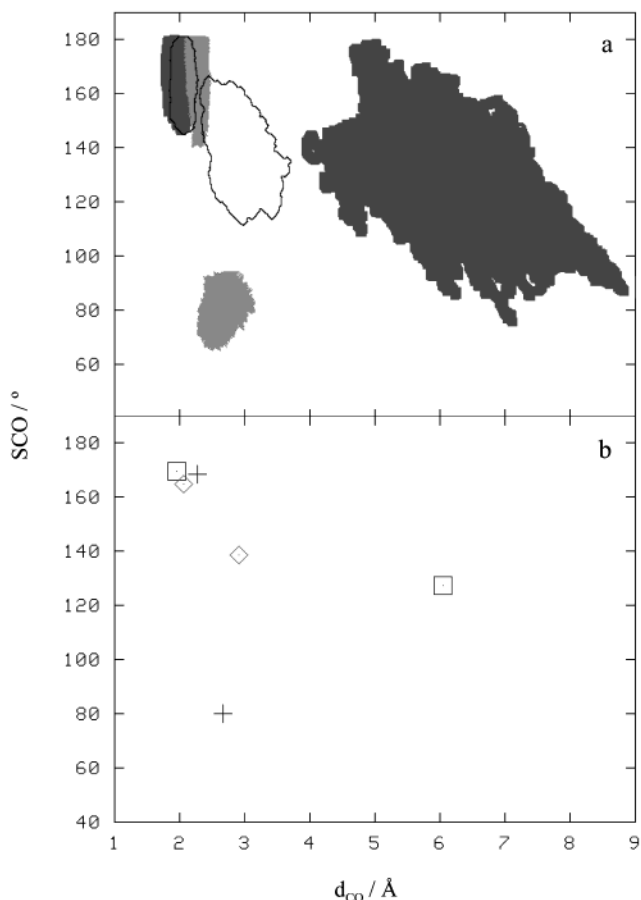


**Figure 5.** (a) QM/MM trajectories ( $C\cdots O$  distance in Å and  $S\cdots C\cdots O$  angle in degrees) corresponding to reactants' free-energy minima and transition structure of the transmethylation reaction obtained in a vacuum (light gray area), solution (dark gray area), and COMT (contour line area). (b) Averaged values of the represented internal coordinates for trajectories in gas phase (+), solution (□), and COMT (◇) corresponding to the transition structure and the reactants of the reaction.

observed for the Menschutkin reaction.<sup>44</sup> This result demonstrates the importance of using TS structures located in the enzyme or solution rather than those obtained from calculations in a vacuum. The distribution of structures corresponding to the MC in the enzyme is much closer to the TS distribution than that for either the vacuum or water reactant complexes. This proximity reflects the preorganization of the enzyme that favors binding of reactants in the MC geometry. The gas-phase reactant-complex distribution has  $d_{CO}$  distances similar to those for the enzyme but with  $SCO$  angles far from linearity. The SSIP in water is more flexible and shows large amplitude movements. On average, both the  $d_{CO}$  distance and the  $SCO$  angle in solution are less favorable for the reaction than in the enzyme. Obviously, the resemblance of the enzymatic reactants to the TS is related with the lower free-energy barrier found in this case.

**Solvation Energy and Solvent Reorganization.** Since the reaction involves annihilation of charges in going from reactants to products, a polar medium like water stabilizes reactants better than the TS; the solute–solvent interaction energy is greater

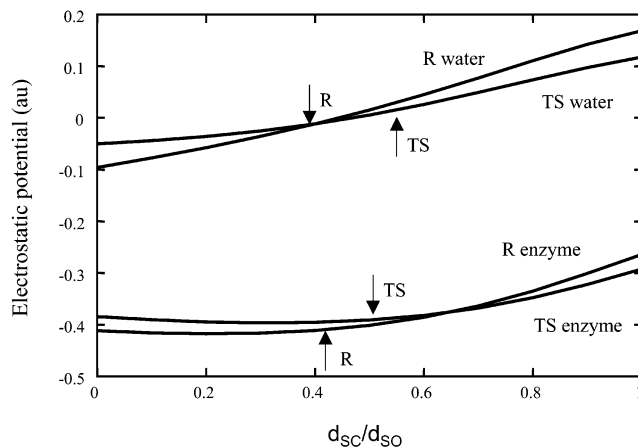


**Figure 6.** Plot of averaged electrostatic potential against the fractional degree of methyl transfer, along the vector connecting the donor S and acceptor O atoms, due to the charge distribution of the MM environments (QM atoms excluded), obtained from all geometries of either the reactant complex (R water, R enzyme) or the TS (TS water, TS enzyme) trajectories, for both water and enzyme environments.

for the reactants than for the TS, and therefore aqueous solvation raises the reaction energy barrier relative to that in a vacuum. Solvation involves not only a favorable solute–solvent interaction, but also an unfavorable reorganization of the solvent itself. Since the solvent structure is more broken when interacting with the reactants than with the TS, the solvent reorganization energy is greater for the reactants than for the TS. However, it is smaller in magnitude than the solute–solvent interaction energy: in continuum solvation models the reorganization energy is equal to minus one-half of the interaction energy.<sup>4</sup> Thus, solvent reorganization energy tends to offset the increase in the reaction barrier due to solvation. As noted above, there is also an unfavorable free-energy change in aqueous solution of about 7 kcal mol<sup>-1</sup> in going from the SSIP to the MC-like contact ion pair for exactly the same reasons.

**Analysis of Electrostatic Factors in Catalysis.** To show the different electrostatic behavior of the enzyme with respect to the aqueous solution, we have studied the electrostatic potential created by the MM regions in these two environments, as an alternative analysis to the one presented by Warshel and co-workers.<sup>45</sup> The reaction may be considered as the transfer of a positive charge, on the transferring methyl group, from the S atom of SAM to the O<sup>-</sup> of catecholate. Of course, this is intrinsically a favorable process from the electrostatic point of view. The question is whether the environment within which the reaction occurs helps or hinders the transfer of positive charge. To answer this, we have evaluated the averaged electrostatic potential experienced by a unit positive charge, located at positions along the vector connecting the donor S and the acceptor O atoms, due to the charge distribution of the MM environment (QM atoms excluded), in all the geometries of either the trajectories of reactant complex (“R water”, “R enzyme”) or the trajectories of TS (“TS water”, “TS enzyme”), for both water and enzyme environments. Figure 6 is a plot of the electrostatic potential versus the fractional degree of methyl transfer ( $d_{SC}/d_{SO}$ ); the two values of this coordinate corresponding to the reactant complex and TS are marked on the plot. A negative value of the electrostatic potential indicates an attractive

(44) (a) Solà, M.; Lledós, A.; Durán, M.; Bertrán, J.; Abboud, J. L. M. *J. Am. Chem. Soc.* **1991**, *113*, 2873–2879. (b) Gao, J.; Xia, X. *J. Am. Chem. Soc.* **1993**, *115*, 9667–9675. (c) Dillet, V.; Rinaldi, D.; Bertrán, J.; Rivail, J. L. *J. Chem. Phys.* **1996**, *104*, 9437–9444.

(45) Florian, J.; Goodman, M. F.; Warshel, A. *J. Phys. Chem. B.* **2002**, *106*, 5739–5753

interaction between the +1 probe charge and the MM environment, whereas a positive value indicates a repulsive interaction. Inspection of the “R water” curve shows a steep rise from a small negative electrostatic potential at  $d_{SC}/d_{SO} = 0$  to an appreciably positive value at  $d_{SC}/d_{SO} = 1$ : the charge distribution within the MM environment of the solvent water molecules is well suited for stabilization of the dipolar reactant complex but badly matched to the (neutral) product complex. The same trend is shown by the “TS water” curve, but with a markedly smaller slope at each point, since the charge distribution of the environment is complementary to a less-dipolar substrate. Clearly the electrostatic potential of the environment is a hindrance to the transfer of “CH<sub>3</sub><sup>δ+</sup>” from S to O<sup>-</sup> in water. In this simple model (neglecting interactions between QM atoms), the work required for methyl transfer is the product of the partial positive charge  $\delta q$  multiplied by the electrostatic potential difference  $\Delta V$ .

$$W = \delta q \times \Delta V \quad (4)$$

The curves for “R enzyme” and “TS enzyme” are very similar, both indicating an attractive electrostatic interaction with the protein environment for the probe charge located at the position of the transferring methyl in both the reactant complex and the TS, and both changing to a repulsive interaction in the product complex. The electrostatic potential difference between the reactant complex and the TS is much smaller in the enzyme active site than in water. Moreover, the similarity of the electrostatic potentials at the values of  $d_{SC}/d_{SO}$  corresponding to the reactant complex and to the TS shows that the enzyme does not undergo any significant structural reorganization as the reaction proceeds to the TS. The electrostatic field created by the enzyme is mainly due to a permanent charge distribution, and thus, it remains essentially unaltered and in a favorable orientation as the reaction proceeds. In contrast, the reaction field in water reflects the polarization of the solvent induced by the change in the solute polarity.

We have also computed the electrostatic field vector ( $\bar{E}$ ) at the position of the C atom of the transferring methyl group, using the structures of the reactant complex and TS obtained in solution and in the enzyme active site. We find that the averaged magnitude of  $\bar{E}$  calculated in the enzyme ( $\langle |\bar{E}|_{\text{enzyme}} \rangle \approx 0.08$ ) is larger than that obtained in solution ( $\langle |\bar{E}|_{\text{water}} \rangle \approx 0.05$ ). Also, while the modulus of  $\bar{E}$  and the magnitude of its projection on the S–O direction are essentially coincident in aqueous solution, owing to the homogeneous nature of this medium, in the enzyme, the magnitude of the S–O component of  $\bar{E}$  is much lower ( $\approx 0.01$ ) than the magnitude of  $\bar{E}$  itself. This result means that the electrostatic field is less unfavorable to the transfer of a positive charge from S to O in the enzyme than in aqueous solution. We conclude that the enzyme is already preorganized to favor the reaction of SAM with catO<sup>-</sup>, relative to the same process in water, and the much smaller amount of reorganization of the protein environment, relative to the aqueous environment, in proceeding from the reactant complex to the TS, leads to a diminution of energy barrier to reaction.

**Analysis of Interaction Energies.** These results are also confirmed by the analysis of the contribution of the solute–solvent or substrate–enzyme interaction energy to the potential energy barrier. We have estimated these energy contributions by means of 500 ps MD simulations for the TS and reactive

reactants in both media. In aqueous solution, the value obtained for the change of the interaction energy from reactants to TS is 45.7 kcal mol<sup>-1</sup> and is dominated by the electrostatic component of 46.5 kcal mol<sup>-1</sup>. In the enzyme, the interaction energy contribution to the potential energy barrier is 32.6 kcal mol<sup>-1</sup>, with the electrostatic component being only 30.4 kcal mol<sup>-1</sup>. This result confirms the fact that the enzyme environment requires less energy deformation to proceed from reactants to TS than the water solvent.

In a recent review, Warshel and Parson<sup>43c</sup> have commented upon the MD simulations and QM calculations of Bruce and co-workers<sup>19b,c</sup> for COMT. In response to the suggestion that the enzyme does not preferentially stabilize the TS relative to the MC, they proposed that calculations for the same reaction in water would show that the TS is much more stable in the enzyme than in solution. Our calculations provide confirmation of this proposal: aqueous solvation and the COMT active site both stabilize the reactants more than the TS, but the TS is less destabilized by the enzyme than by water.

## Conclusions

A theoretical study of the reaction catalyzed by the catechol *O*-methyltransferase compared with the same reaction in solution has been carried out by a combination of hybrid QM/MM optimizations and statistical simulations. The two factors previously proposed as important contributions to rate enhancement in enzymatic processes, reorganization and preorganization, of enzyme, substrates and solvent, have been identified for the bimolecular reaction here studied. The main characteristic of this S<sub>N</sub>2 reaction is that oppositely charged reactants combine to generate neutral products, so an initial polar moment is annihilated as the reaction advances. An electric field thus stabilizes the reactants preferentially to the TS. Nevertheless, there is a big difference between aqueous and enzymatic environments. In solution, the TS is destabilized with respect to the reactants for two reasons: (i) the polarity of the solute diminishes, and (ii) consequently, the reaction field is also decreased. Following a continuum model description, the interaction energy depends on the product of the solute polarity (dipole moment) and the magnitude of the reaction field. This last, in turn, is a function of the solute dipole moment. Thus, the TS destabilization, relative to the reactants, is a function of the square of the change in solute polarity.

$$\Delta E \propto \Delta(\bar{R} \cdot \bar{\mu}) \propto \Delta\mu^2$$

In the enzyme, insofar as the electric field is mainly a permanent field and that our analysis indicates only a small reorganization of the protein environment, the variation of the interaction energy would be only a function of the variation of the substrate polarity:

$$\Delta E \propto \bar{E} \cdot \Delta\bar{\mu}$$

Therefore, destabilization of the TS is expected to be lower than in solution and the activation barrier will be smaller. On the other hand, the substrate preorganization can be also understood using the same arguments. In aqueous solution, the reaction field stabilizes those reactants with larger charge separation (large carbon–oxygen distance, large dipole moment) and consequently is less similar to the TS. In the enzyme, the permanent field, already prepared to stabilize the TS, will obviously

stabilize those reactant structures oriented in TS-like manner, reactive to reactants.

In our opinion, the connection we have found between the environment reorganization and substrate preorganization is a general feature of enzymatic processes. The structure of the enzyme is designed to favor the TS relative to the reactant *compared* to the in solution process. This enzyme structure is flexible enough to accommodate different conformers of the reagents and TSs, but deformation of the enzyme involves an energetic penalty. When going from reactants to TS, the enzyme deformation will be as small as possible (small enzyme reorganization), selecting, consequently, those reactant conformers resembling the TS (substrate preorganization). Thus, reorganization and substrate preorganization are two related effects having a common origin in the enzyme structure (or enzyme preorganization) that stabilizes the TS. In conclusion, the main

factor of enzyme catalysis is found in the enzyme structure, which is the product of a long evolution whose target is the complementarity with the TS structure of the reaction to be catalyzed. As a consequence, the enzyme would select those reactant conformers resembling the TS, what we call substrate preorganization.

**Acknowledgment.** We are indebted to DGI for project DGI BQU2000-C03, BANCAIXA for project P1A99-03, and Generalitat Valenciana for project GV01-324, which supported this research, and the Servei d'Informatica of the Universitat Jaume I for providing us with computer capabilities. M.R. thanks the Spanish Ministerio de Educación, Cultura y Deporte for a doctoral fellowship. S.M. thanks UJI-BANCAIXA Foundation for a Postdoctoral fellowship.

JA0299497